([1, 10]). However, the implementation of a teleoperation system with force feedback presents outstanding obstacles, such as force measurement/estimation, transparency, stability and others ([11–13]).

The aforementioned commercial systems are specialized for a particular technique or medical application, being difficult to integrate with other systems. Therefore, versatile and modular medical robotic systems are needed, which be able to perform diverse interventions. This variety must be achieved while at the same time keeping the safety and benefit of the patient as central goal. Some examples of robotic research (non-commercial) platforms aimed to provide flexibility and versatility are the MiroSurge ([14]) and the KIT robotic platform ([15, 16]).

In this line of thought, we have established as main purposes of our development the high adaptability of the robotic platform to explore different applications and its easy integration with other systems, providing, in any case, high performance. We plan to explore applications related to medical image acquisition during surgery, patient registration, and surgical/medical equipment operation.

In this paper we briefly describe the implementation of the platform's teleoperation and path following modes from a general purpose perspective. Also, we discuss relevant aspects of the system, as well as future directions and application fields to be investigated.

2. Materials and Methods

2.1 System Description

The system is composed by a KUKA LWR IV+ robotic arm, a haptic device and a remote computer where the software to command the robot is executed. The developed software allows simulating and commanding the real robot, in any case providing the visualization of a virtual scene with the current state of the robot. There are two operation modes: teleoperation (master-slave scheme) and path following.

2.1.1 Robotic Arm

The KUKA LWR IV+ (KUKA Roboter GmbH, Augsburg, Germany) ([17]), shown in Figure 1, is a 7-joint lightweight robot specially equipped with torque sensors to enable a compliant behavior. The robot controller allows the implementation of various control modes, which include, besides the typical position control, Cartesian and axis-specific impedance schemes. By adjusting the stiffness and damping parameters of the impedance control, interesting dynamic behaviors can be obtained, such as the gravity compensation mode (also known as hands-on mode). In this approach the operator moves the robot freely with his hands as a joint-level torque controller sustains the weight of the robot. This greatly facilitates the interaction of robots and humans (see reference [18] for a practical application).

Also, the robotic system is able to provide an estimation of the force that is being exerted at the tip of the REE.

Using the KUKA Fast Research Interface (FRI) the robot controller can establish communications with a remote PC using UDP protocol. The FRI provides a C++ interface of high level instructions, which can be used to retrieve information of the robotic arm, such as the REE Cartesian position and orientation, and to implement different control strategies.

Figure 1. KUKA LWR IV+ lightweight robot ([17]) embedded to a surgical bed.

2.1.2 Haptic Device

In this context, these mechatronic devices are used to capture the movement commands in the teleoperation mode of the robotic platform, i.e., they are the master consoles. Additionally, they can exert forces to the surgeon hands, thus providing force feedback. Our development currently supports Omega6 and Omega7 devices from Force Dimension (Force Dimension, Nyon, Switzerland). Figure 2 depicts the Omega6 haptic device.

2.1.3 Software

The developed software uses the open source H3D API (SenseGraphics AB, Kista, Sweden) to perform the graphic and haptic rendering within the same framework. The virtual scenes are defined using the X3D standard for representing 3D computer graphics. The graphic rendering is performed using OpenGL, which is also a standard in the computer graphics industry. This API has been written in C++, designed to be cross-platform and supports a wide spectrum of haptic devices.

Our application is completely written in C++. Through the development of a proper class hierarchy, we are able to simulate the behaviour of the robot and to command the real robot, using various operation modes in a modular and efficient way. These operation modes can be switched at any time.

Depending on the mode of operation of the system, the robot 3D model is updated according to the results of the inverse kinematics (IK) computation or retrieving the joints' angles using the FRI.

A typical scene in our application can include, besides a model of the robotic arm, a virtual reality representation of the haptic device's stylus, a model of the patient and other objects of interest, such as forbidden region virtual fixtures (FRVF). The virtual scene intends to represent the real scene precisely. Note that this step requires accurate registration methods, especially to determine the patient position with respect to the WCS.

The user can configure the different parameters related to the operation of the system using a graphic user interface, which was built using the open source wxWidgets API.

Figure 2. Omega6 haptic device from Force Dimension.

2.2 Operation Modes

This subsection aims to describe the implementation of the teleoperation and autonomous path following modes. First, the solution to the inverse kinematics is addressed, since this is a necessary step to simulate the robot, or to command it when the joint position control is used. Next, the teleoperation and autonomous path following modes are discussed.

2.2.1 Inverse Kinematics

Given a desired position and orientation $\boldsymbol{T}_r$ of the robotic manipulator's end-effector, it is necessary to calculate the configuration of the angles of the robot's joints $\boldsymbol{q}$ that allows it to reach $\boldsymbol{T}_r$. Note that $\boldsymbol{T}_r$ has a translational component (x, y, z) and a rotational component (a, b, c), which follows the Euler's angles convention. The set of angles of the joints of the robotic arm is defined as $\boldsymbol{q}=\{\theta_1, \theta_2, \ldots, \theta_n\}$ where n is equal to the number of joints of the manipulator.

There are several approaches to solve this problem, including analytic ([19]) and numeric methods ([20]). Since the robot we deal has a redundant joint (7-DOF), the adopted solution method is based on the Jacobi matrix $J(\boldsymbol{q})$ of the robot.

Here, matrix $J(\boldsymbol{q})$ establishes a relationship between the REE's velocities in the Cartesian space (task space) $\dot{\boldsymbol{X}}_r$ and the velocities of the robot's joints $\dot{\boldsymbol{q}}$, as shown in equation 1

$$\dot{\boldsymbol{X}}_r = J(\boldsymbol{q})\dot{\boldsymbol{q}} \tag{1}$$

where $\dot{\boldsymbol{X}}_r=\{\dot{x}, \dot{y}, \dot{z}, \dot{a}, \dot{b}, \dot{c}\}$ describes the linear velocity $(\dot{x}, \dot{y}, \dot{z})$ and angular velocity $(\dot{a}, \dot{b}, \dot{c})$ of the REE with respect to the robot's LCS. Then, column i $(1 \leq i \leq n)$ of $J(\boldsymbol{q})$, represented by $\boldsymbol{J}_i$, describes how a change in angle $\theta_i \in \boldsymbol{q}$ affects each component of $\dot{\boldsymbol{X}}_r$, as shown in equation 2.

$$\boldsymbol{J}_i^T = \left[\frac{\partial x}{\partial \theta_i} \quad \frac{\partial y}{\partial \theta_i} \quad \frac{\partial z}{\partial \theta_i} \quad \frac{\partial a}{\partial \theta_i} \quad \frac{\partial b}{\partial \theta_i} \quad \frac{\partial c}{\partial \theta_i}\right] \tag{2}$$

Each one of the entries of $\boldsymbol{J}_i$ can be obtained geometrically, as shown in reference [21].

From equation 1, it can be obtained that:

$$\Delta\boldsymbol{q} = J(\boldsymbol{q})^{-1}\Delta\boldsymbol{X}_r \tag{3}$$

by discretizing for some given sampling period t. Then, if $\Delta\boldsymbol{X}_r$ is replaced by the vector $\boldsymbol{e}$, which is defined by $\boldsymbol{e}=\boldsymbol{T}_r - \boldsymbol{X}_r$ (the difference between the desired and the current REE pose) in equation 3, the necessary $\Delta\boldsymbol{q}$ to reach $\boldsymbol{T}_r$ is obtained.

Note that in our case $J(\boldsymbol{q})$ is a 6x7 matrix; then it is not invertible. In the literature there are several methods to solve this problem. It worth mentioning that even if $J(\boldsymbol{q})$ were square, it is not always invertible, due to the occurrence of singularities. One of the solutions is to implement the pseudo inverse method ([22]). An interesting feature of this approach is that it allows taking advantage of the nullspace of $J(\boldsymbol{q})$. This means that the angles of the robot's joints can be configured in a different way while $\boldsymbol{X}_r$ remains unchanged. This is important in the surgical theatre, since there are space constraints and multiple objects to avoid. However, this method tends to be unstable when the robot is near a singularity.

Other method is the use of the transpose of $J(\boldsymbol{q})$ ([21]), which is computationally less expensive than the pseudo inverse approach and more stable, but it may converge slower and does not take advantage of the redundancy of the robot.

In any case, the results are improved by restricting the maximum linear displacement and rotation described by $\boldsymbol{e}$ ([20]). To illustrate this concept, let $\boldsymbol{e}_p$ be the translational component of $\boldsymbol{e}$ and d the value of maximum linear displacement. If $\|\boldsymbol{e}_p\| \leq d$, then $\boldsymbol{e}_p$ is not modified. Otherwise, $\boldsymbol{e}_p = \hat{\boldsymbol{e}}_p * d$, and $\boldsymbol{T}_r$ is reached in several iterations. In an analogous way the rotation component $\boldsymbol{e}$ of can be restricted. Also, it is critical to monitor the resulting joint speeds and limit them.

2.2.2 Teleoperation

A telesurgical system with force feedback capability consists of a human operator (surgeon), a master device, a communication channel, a bilateral controller, a slave

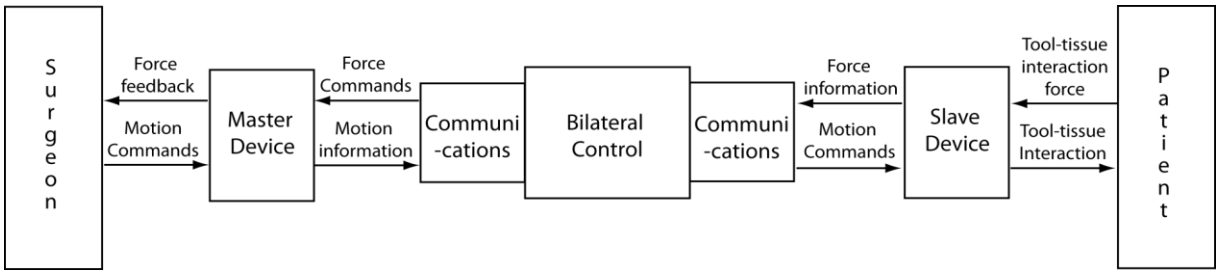

Figure 3. General scheme of a telesurgical system with force feedback.

manipulator and a remote environment (patient) ([23]).

This system and the workflow of information among its components are depicted in Figure 3.

In order to illustrate the following concepts, let us define X_h, X_{hw}, T_r and T_{rw} as the matrix representation of $\boldsymbol{X}_h$, $\boldsymbol{X}_{hw}$, $\boldsymbol{T}_r$ and $\boldsymbol{T}_{rw}$, respectively, using homogenous coordinates.

In our implementation, the master device captures the surgeon's movement commands. This means that the position and orientation of the haptic device's stylus $\boldsymbol{X}_h$ are used to define $\boldsymbol{T}_{rw}$. Note that the workspace and local coordinate systems of the haptic device and slave robot may be very different; therefore, a transformation matrix M_{hw} needs to be applied to the measurements X_h to obtain the desired pose with respect to a common coordinate system (world), which is equivalent to $X_{hw}= M_{hw}X_h$. In this way, T_{rw} can be assigned as $T_{rw}=X_{hw}$ and the transformation matrix M_{rw}^{-1} is used to transform the commands T_{rw} to the robot's local coordinate system $T_r=M_{rw}^{-1}T_{rw}$. A scaling factor may be applied between X_{hw} and T_{rw}, in order to miniaturize the movements commanded by the surgeon, taking in account that the procedure to perform this is different for the linear and rotational components. To guarantee that the operation speed is safe, the translational and rotational components of $\boldsymbol{e}=\boldsymbol{T}_{rw}-\boldsymbol{X}_{rw}$ are limited as described before.

Depending on the application (and safety conditions), the desired $\boldsymbol{T}_{rw}$ can be set as the reference for the Cartesian position controller of the robot, or used to compute the inverse kinematics and then use the joint-position controller.

With respect to the force feedback, the estimated force resulting from the interaction of the REE with the patient is transformed to the world and local haptic coordinate system to produce the desired results. Before reflecting the mentioned interaction force to the surgeon a scaling factor may be applied to the measured values.

The force feedback that is provided to the surgeon, can include, in addition to information of real interactions (e.g. tool-tissue contact force), computer-generated forces. These virtual forces, also known as virtual fixtures, help to improve the operation of telerobotic system ([24]). Virtual fixtures can be classified as Guidance Virtual Fixtures (GVF) or Forbidden-Region Virtual Fixtures (FRVF) ([9]). GVF help the surgeon to perform a movement along a defined path, while FRVF prevent the surgeon accessing a specific region of interest ([25]).

Figure 4 shows an example of a simple FRVF implementation, which acts like a wall in the world's XZ plane, limiting the surgeon's workspace along the world's Y-axis. A 3D model is used in the virtual environment to represent the haptic device's stylus, whose geometry, in this case, corresponds to the tool that is manipulated by the slave robot. The collisions of the virtual stylus with the other objects of the virtual scene produce reaction forces. These reaction forces may correspond to rigid or compliant interactions, which can additionally recreate surface properties, such as friction and texture.

Summarizing, in the FRVF implementation a contact force will be calculated and delivered to the surgeon when the haptic device's virtual representation touches the virtual fixture. In this way, neither the haptic device's stylus nor the REE can move beyond the virtual wall. Figure 4(b) shows the position of the REE while Figure 4(c) displays the X, Y and Z components of the force that was transmitted to the surgeon. Since the REE follows the position and orientation of the haptic device's stylus, they occupy the same space, and therefore they cannot be distinguished from each other in Figure 4(a). Note that Figure 4(b) shows how the movement of the REE is constrained along the Y-axis, and how this situation is related to the force feedback depicted in Figure 4(c). As a consequence of this implementation, a mixed reality is created, given that feedback from real and virtual interactions are provided to the surgeon.

More complex geometries can be used to define a FRVF. For example, an organ 3D model can be used to encapsulate the patient's real organ, avoiding undesired interactions between the slave robot and critical anatomical structures. The 3D reconstruction can be obtained from the preoperative patient's images as described in reference [26], in order to achieve a high level of realism. It worth mentioning, that the proper functionality of this feature depends of a correct registration of the patient and his/her reconstructed preoperative 3D organs models.

The described implementation of the teleoperation mode (position forward-force feedback control) is suitable for the available hardware. However, according to the needs related to the application and medical techniques, it is possible to find different approaches in the existing literature. For example, the system implemented by

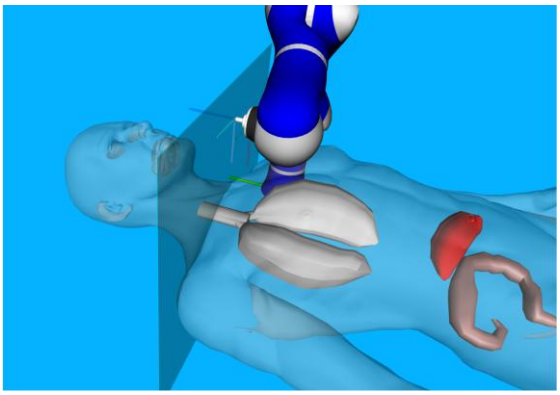

a)

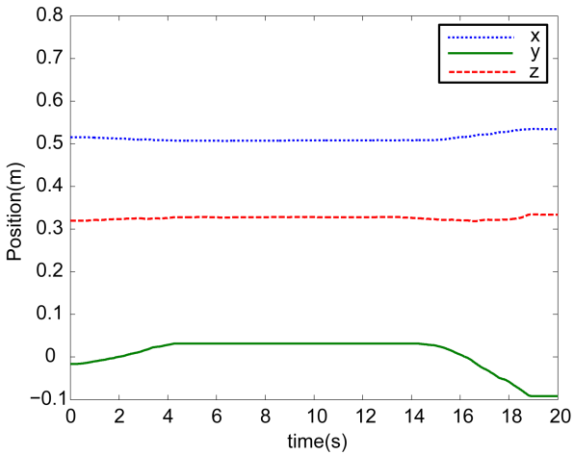

b)

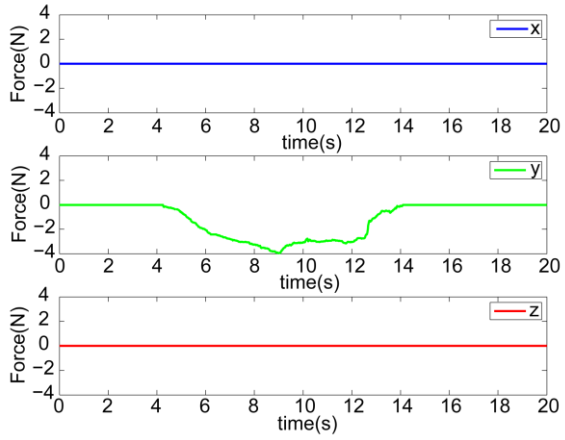

c)

Figure 4. (a) Interaction of the KUKA robot ([17]) with a FRVF in the XZ plane. (b) REE position vs. time. (c) Rendered contact force vs. time.

reference [27] considers the case of a kinematic correspondence between the master and slave systems. This means that the surgeon commands the movements of each joint of the slave robot individually. This implies that the IK computation is not necessary.

2.2.3 Path Following

It is possible to generate trajectories composed by parametric curve segments for the robotic arm. The required orientation of the REE at the initial and final points of each segment can be defined independently of the path, allowing different configurations in a flexible fashion.

The described trajectories are resampled according to the desired precision to traverse them by defining a sampling distance u. This means that the original path is approximated in a piecewise linear way. Thus, each segment of the trajectory is described by M number of poses, which is different for each case. The set $Q = \{\boldsymbol{Q}_1, \boldsymbol{Q}_2, \ldots, \boldsymbol{Q}_M\}$ constitutes the resulting discretized trajectory of a particular segment. Each $\boldsymbol{Q}_i$ ($\boldsymbol{Q}_i \in Q$) is a vector that describes the i–th desired pose of the RRE with respect to the WCS where $1 \leq i \leq M$. Analogously, the orientation of the REE at each $\boldsymbol{Q}_i$ is determined performing a linear interpolation of the total rotation matrix R_T, defined by $R_T = R_M R_1^{-1}$, where R_M and R_1 correspond to the matrix representation of the rotation parts of $\boldsymbol{Q}_M$ and $\boldsymbol{Q}_1$ respectively. This means that R_T is applied in $M - 1$ steps, which can be done easily using quaternion notation.

Each $\boldsymbol{Q}_i$ is used as a reference for the robot controller $\boldsymbol{T}_{rw}$. When $\boldsymbol{e} = \boldsymbol{T}_{rw} - \boldsymbol{X}_{rw}$ is below some predefined threshold, $\boldsymbol{T}_{rw}$ is assigned as $\boldsymbol{T}_{rw} = \boldsymbol{Q}_{i+1}$, and the process is repeated until the total Q set is traversed. In this way, all the segments that compose the desired trajectory are processed.

The poses that compose the trajectory's segments can be obtained from several sources, such as medical images or by using the robot's hands-on mode. Figure 5 shows the simulation of the robotic arm following a simple trajectory.

3. Applications

The objective of this section is to give a brief overview of some of the applications we plan to develop in the near future and a use case of the platform.

3.1 Augmented Reality

We plan to extend the platform with the augmented reality prototype for endoscopic view developed by our team ([28]).

In this way, besides developing an automatic positioning system for the endoscope, we could provide an endoscopic view enhanced by the overlay of organs' 3D models in real-time. Thus, the surgeon is provided with valuable information to ease the identification of the structures of interest during the intervention. In this

implementation we can also explore automatic calibration and registration methods for the augmented reality system. Similar setups can be used for other applications, such as real-time surface reconstruction to obtain 3D models of the patient during surgery.

3.2 Ultrasound Image Acquisition

We are currently extending our hardware with ultrasound probes. The goal is to provide the surgeon with real-time ultrasound images, during the surgery, to support the decision process.
The positioning of the ultrasound probe can be automatic or teleoperated. In the automatic scenario, the anatomic structure of interest is identified by processing the images. Then, the robot is programmed to maintain in target the relevant region. This process includes the location of the relevant coordinate systems (probe, WCS, patient, region of interest, etc.).

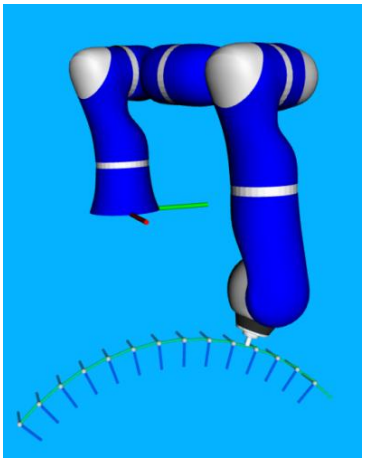

Figure 5. KUKA robot ([17]) in path following mode traversing a single circular trajectory.

3.3 Camera Positioning

Here we present a use case of the platform in path following mode. This development illustrates the preliminary results of the implementation of the robotic platform with simple and known image acquisition equipment (conventional camera). In this way, the proper performance of the system can be verified easily.

Interest points extraction and matching is a critical task for many computer vision applications. Currently, several new mechanisms for key point extraction and for feature description are emerging, so normalized data and evaluation protocols are needed in order to assess them accurately. In order to obtain a set of images with perspective distortion that allows the appraisal of the mentioned mechanisms, we used a Canon 7D camera attached to the robotic arm to generate different points of view of the same target. The use of the path following mode of the robotic platform allowed us to generate known, repeatable and precise poses and trajectories around the target scene (see Figure 6). The details of this research work are presented in other manuscript, which is under review process for publication.

With the capability of the system verified, the application fields can be extended to manipulate ultrasound probes, endoscopes and other medical equipment, taking advantage of the high position accuracy and repeatability provided by the system.

4. Discussion

In this section we aim to discuss important aspects related to the presented implementation and to the current state of the art of these systems.

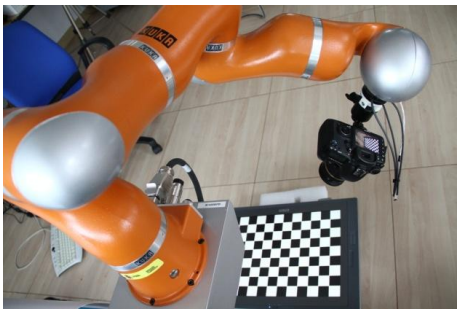

Figure 6. KUKA robot ([17]) in path following mode during the image acquisition process.

4.1 Simulation

As we mentioned before, in order to simulate the robot behaviour in any of the operation modes, it is necessary to solve the kinematics of the manipulator. However, the dynamics of the robotic arm must be considered to provide a realistic simulation.

In order to determine the required actuator torques and forces that allow the manipulator to follow a desired trajectory, the inverse dynamics problem must be addressed. On the other hand, to find the motion (position, velocity, acceleration) of the manipulator as a function of time when driving forces and external loads are applied, it is necessary to solve the forward dynamics problem.

In any case the inertial and mass properties of the manipulator need to be known. If this data is not provided by the robot's manufacturer, they can be estimated from online measurements of the joint torques and manipulator kinematic state ([29]).

4.2 Teleoperation

Previously, we have described the implementation of a position forward-force feedback control scheme for the teleoperation mode of the robotic platform. However, there are other approaches that improve the transparency of the teleoperated systems. Some of them can be found in reference [13]. Ideally, these bilateral control algorithms should provide high transparency and stability. However,

it is difficult to achieve both goals simultaneously, since it requires to eliminate the uncertainties of the control model and the exact implementation of the control laws ([13, 30]).

When a significant time delay is present in the communication among the different components of the system, the complexity of achieving a proper behavior is increased. Several approaches have been proposed to address this problem; most of them are based on the passivity framework ([31, 32]). In this scheme, stability is guaranteed if each component of the system behaves passive (does not increase the system's energy) ([14, 33]). A valuable work in this topic is presented by Zhu et al. in [33], which provides a survey of the main control approaches for bilateral teleoperation with time delay, reviewing the advantages and weaknesses of passivity based, prediction based and sliding-mode control schemes.

4.3 Registration

An accurate registration between the patient, robotic arm, tracking devices and other relevant systems is critical to perform a successful intervention. For this process, electromagnetic or optical tracking systems are commonly used. In procedures such as osteotomies, the markers that allow tracking the patient can be rigidly attached to his/her bones ([18]). When the target of the intervention is an organ that suffers significant deformation, the mentioned method is not a plausible option to perform its registration and tracking. In this case, one of the technologies that could be explored to perform a real-time registration is ultrasound ([34]).

4.4 Force Measurement

We are currently able to retrieve information about the force exerted by the REE through the FRI. The obtained data is estimated using the measurements of the torque sensors installed at the robot's joints. Nevertheless, the accuracy of this estimation is impaired when the robot approaches to singular configurations.

One of the alternatives to address this problem is to attach a force sensor to the tool handled by the robot. Nonetheless, space constraints, sterility requirements, proper placement of the sensing element and costs need to be to assessed when integrating force/torque sensors to surgical instruments or to other medical equipment ([35]).

For MIS procedures the fulfillment of these requirements is particularly difficult due to the nature of these techniques. Puangmali et al. in [12] discuss the design considerations of installing force and tactile sensors to MIS surgical instruments, introducing also a review of the recent advances in sensing technologies and methods.

4.5 Path Planning

In order to provide the robotic platform with autonomous capabilities, information concerning its environment must be provided. The use of cameras to accomplish this task has been widely adopted, due to the great amount of information that can be extracted from a single source.

Image processing techniques are needed to detect the goals and possible obstacles that the manipulator may find when performing a task. Then, this information is used to plan a trajectory that avoids collisions and reaches the target safely.

As of today, there are powerful software packages and libraries to perform the mentioned constrained path planning, such as OpenRAVE ([36]). The integration of these packages to our system would supplement the capability to follow user-defined trajectories.

5. Conclusion and Future Work

We have presented a prototype of a robotic research platform that allows the implementation of novel applications in the field of image-guided surgery.

In this paper we have focused in describing the implementation of the teleoperation and path follow up modes of the platform, which constitute the base for future developments. Also, we have presented some of the applications to be addressed in the near future, as well as an application of the path-follower module.

Finally, we discuss the current status of, and possible solutions to, outstanding issues connected to the robotic platform, such as: (1) simulation, (2) teleoperation, (3) registration, (4) force measurement, and (5) path planning.

Future work includes:

1. Improvement of resolution and accuracy of tool-tissue force estimation/measurement.
2. Implementation of high-performance bilateral control schemes for improvements of transparency and telepresence. In particular, it is interesting to address the problem of bilateral teleoperation under significant time delay.
3. Integration of optical and electromagnetic trackers to improve the accuracy of position and orientation measurements.

References

[1] E. Westebring-Van Der Putten, R. Goossens, J. Jakimowicz, and J. Dankelman, Haptics in minimally invasive surgery-a review, *Minimally Invasive Therapy & Allied Technologies*, *17*(1), 2008, 3–16.

[2] D. B. Camarillo, T. M. Krummel, J. K. Salisbury, and others, Robotic technology in surgery: past, present, and future, *The American Journal of Surgery*, *188*, 2004, 2–15.

[3] T. Haidegger and Z. Benyó, Industrial Robotic Solutions for Interventional Medicine, *Proc. International GTE Conference MANUFACTURING*, Budapest, 2008, 125–130.
[4] P. Gomes, Surgical robotics: Reviewing the past, analysing the present, imagining the future, *Robotics and Computer-Integrated Manufacturing*, *27*(2), 2011, 261–266.
[5] U. Hagn, T. Ortmaier, R. Konietschke, B. Kubler, U. Seibold, A. Tobergte, M. Nickl, S. Jorg, and G. Hirzinger, Telemanipulator for remote minimally invasive surgery, *Robotics & Automation Magazine, IEEE*, *15*(4), 2008, 28–38.
[6] S. L. Lee, M. Lerotic, V. Vitiello, S. Giannarou, K. W. Kwok, M. Visentini-Scarzanella, and G. Z. Yang, From medical images to minimally invasive intervention: Computer assistance for robotic surgery, *Computerized Medical Imaging and Graphics*, *34*(1), 2010, 33–45.
[7] A. Simorov, R. S. Otte, C. M. Kopietz, and D. Oleynikov, Review of surgical robotics user interface: what is the best way to control robotic surgery?, *Surgical Endoscopy*, 2012, 1–9.
[8] G. S. Weinstein, B. W. O'Malley Jr, S. C. Desai, and H. Quon, Transoral robotic surgery: does the ends justify the means?, *Current opinion in otolaryngology & head and neck surgery*, *17*(2), 2009, 126-131.
[9] T. Yamamoto, N. Abolhassani, S. Jung, A. M. Okamura, and T. N. Judkins, Augmented reality and haptic interfaces for robot-assisted surgery, *The International Journal of Medical Robotics and Computer Assisted Surgery*, *8*, 2011, 45–56.
[10] M. Tavakoli, R. Patel, and M. Moallem, A haptic interface for computer-integrated endoscopic surgery and training, *Virtual Reality*, *9*(2), 2006, 160–176.
[11] A. M. Okamura, Methods for haptic feedback in teleoperated robot-assisted surgery, *Industrial Robot: An International Journal*, *31*(6), 2004, 499–508.
[12] P. Puangmali, K. Althoefer, L. D. Seneviratne, D. Murphy, and P. Dasgupta, State-of-the-art in force and tactile sensing for minimally invasive surgery, *Sensors Journal, IEEE*, *8*(4), 2008, 371–381.
[13] M. Tavakoli, A. Aziminejad, R. V. Patel, and M. Moallem, High-fidelity bilateral teleoperation systems and the effect of multimodal haptics, *Systems, Man, and Cybernetics, Part B: Cybernetics, IEEE Transactions on*, *37*(6), 2007, 1512–1528.
[14] U. Hagn, R. Konietschke, A. Tobergte, M. Nickl, S. Jörg, B. Kübler, G. Passig, M. Gröger, F. Fröhlich, U. Seibold, and others, DLR MiroSurge: a versatile system for research in endoscopic telesurgery, *International journal of computer assisted radiology and surgery*, *5*(2), 2010, 183–193.
[15] H. Mönnich, P. Nicolai, J. Raczkowsky, and H. Wörn, A Semi-Autonomous Robotic Teleoperation Surgery Setup with Multi 3D Camera Supervision, *Proc. International Journal of Computer Assisted Radiology and Surgery (CARS 2011)*, 2011, 132–133.
[16] O. Weede, H. Monnich, B. Muller, and H. Worn, An intelligent and autonomous endoscopic guidance system for minimally invasive surgery, *Proc. International Conference on Robotics and Automation (ICRA), 2011 IEEE*, 2011, 5762–5768.
[17] R. Bischoff, J. Kurth, G. Schreiber, R. Koeppe, A. Albu-Schäffer, A. Beyer, O. Eiberger, S. Haddadin, A. Stemmer, G. Grunwald, and others, The KUKA-DLR Lightweight Robot arm-a new reference platform for robotics research and manufacturing, *Proc. 2010 41st International Symposium on Robotics (ISR), and 2010 6th German Conference on Robotics (ROBOTIK)*, 2010, 1–8.
[18] H. Mönnich, D. Stein, J. Raczkowsky, and H. Wörn, A Hand Guided Robotic Planning System for Laser Osteotomy in Surgery, *Proc. World Congress on Medical Physics and Biomedical Engineering*, Munich, Germany, 2009, 59–62.
[19] P. Chang, A closed-form solution for inverse kinematics of robot manipulators with redundancy, *Robotics and Automation, IEEE Journal of*, *3*(5), 1987, 393–403.
[20] S. R. Buss and J. S. Kim, Selectively damped least squares for inverse kinematics, *journal of graphics, gpu, and game tools*, *10*(3), 2005, 37–49.
[21] H. Monnich, H. Worn, and D. Stein, OP sense—A robotic research platform for telemanipulated and automatic computer assisted surgery, *Proc. 2012 12th IEEE International Workshop on Advanced Motion Control (AMC)*, 2012, 1–6.
[22] J. Wang, Y. Li, and X. Zhao, Inverse Kinematics and Control of a 7-DOF Redundant Manipulator Based on the Closed-Loop Algorithm, *International Journal of Advanced Robotic Systems*, *7*(4), 2010, 1-9.
[23] H. I. Son, T. Bhattacharjee, and D. Y. Lee, Estimation of environmental force for the haptic interface of robotic surgery, *The International Journal of Medical Robotics and Computer Assisted Surgery*, *6*(2), 2010, 221–230.
[24] J. Abbott, P. Marayong, and A. Okamura, Haptic virtual fixtures for robot-assisted manipulation, *Robotics Research*, 2007, 49–64.
[25] J. W. Park, J. Choi, Y. Park, and K. Sun, Haptic Virtual Fixture for Robotic Cardiac Catheter Navigation, *Artificial Organs*, *35*(11), 2011, 1127-1131.
[26] A. De Mauro, J. Raczkowsky, M. E. Halatsch, and H. Worn, Virtual Reality Training Embedded in Neurosurgical Microscope, *Proc. Virtual Reality Conference 2009 (VR 2009)*, 2009, 233–234.
[27] Z. Sun, Z. Wang, and S. J. Phee, Towards haptics enabled surgical robotic system for NOTES, *Proc. 2011 IEEE Conference on* Robotics, *Automation and Mechatronics (RAM)*, 2011, 229–233.
[28] A. De Mauro, J. Mazars, L. Manco, T. Mataj, A. Hernandez, and L. Tommaso De Paolis, Intraoperative Navigation System for Spine Surgery, *International Journal of Computer Assisted Radiology and Surgery*, *7*(1), 2012, 19-22.
[29] P. I. Corke and others, *Visual Control of Robots: high-performance visual servoing* (Research Studies Press, 1996).
[30] S. Katsura, W. Iida, and K. Ohnishi, Medical mechatronics–An application to haptic forceps, *Annual Reviews in Control*, *29*(2), 2005, 237–245.
[31] C. Preusche and G. Hirzinger, Haptics in telerobotics, *The Visual Computer*, *23*(4), 2007, 273–284.
[32] K. Ohnishi, Real world haptics and telehaptics for medical applications, *2010 IEEE International Symposium on Industrial Electronics (ISIE)*, 2010, 11–14.
[33] J. Zhu, X. He, and W. Gueaieb, Trends in the control schemes for bilateral teleoperation with time delay, *Autonomous and Intelligent Systems*, 2011, 146–155.
[34] A. J. Hung, A. L. D. C. Abreu, S. Shoji, A. C. Goh, A. K. Berger, M. M. Desai, M. Aron, I. S. Gill, and O. Ukimura, Robotic Transrectal Ultrasonography During Robot-Assisted Radical Prostatectomy, *European urology*, 2012, 341-348.
[35] T. Haidegger, B. Benyó, L. Kovács, and Z. Benyó, Force Sensing and Force Control for Surgical Robots, *7th IFAC Symposium on Modeling and Control in Biomedical System*s, *7*(1), 2009, 401-406.
[36] R. Diankov, *Automated Construction of Robotic Manipulation Programs*, Carnegie Mellon University, Robotics Institute, 2010.